Tensile deformation and failure processes of amine-cured epoxies

Roger J. Morgan, Eleno T. Mones and Wayne J. Steele
Lawrence Livermore National Laboratory, L-338 University of California, PO Box 808, Livermore, California 94550, USA
(Received 3 November 1980)

Evidence is reviewed for the occurrence of microscopic flow under tensile loads in a variety of amine-cured epoxies. The nature of the deformation and failure processes involved in these flow processes are discussed. The slow-crack growth fracture topographies of these epoxies, fractured as a function of temperature and strain-rate, are reviewed, and consist of a rough initiation region, that can contain microvoids and/or fractured fibrils, surrounded by a smooth temperature and strain-rate dependent region. These topographical features are explained by initial course craze formation followed by crack propagation through the craze midrib. The crack then imposes a higher stress field on the craze tip which produces a small plastic zone that results in a smooth fracture topography. Fracture topographies also indicate that shear band propagation can occur in the fracture initiation process. The ductile mechanical response of many of these epoxies together with direct experimental observations from transmission electron microscopy and birefringence studies produce further evidence that flow can occur in these glasses. Both plastic, homogeneous and inhomogeneous deformations can occur. The inhomogeneous deformations can evolve into macroscopic shear bands. The ability of these crosslinked glasses to undergo microscopic flow is discussed in terms of (i) our understanding of their chemical and physical structure and (ii) covalent bond scission.

Keywords Mechanical behaviour; tensile deformation; failure; craze; fracture, epoxies, strain

INTRODUCTION

The need to conserve energy has stimulated increased interest in the use of epoxies as adhesives and matrices for high performance, light weight, fibrous composites used in aircraft, automobiles, and energy storage systems (such as flywheels). The increasing use of epoxies requires greater knowledge of their durabilities in service environments. To predict the durability of epoxies with confidence requires knowledge of their microscopic deformation and failure processes and the relation of such processes to their chemical and physical structure.

The microscopic deformation and failure modes of epoxies have received little attention. Localized plastic flow has been reported to occur by a number of workers during the failure of epoxies[1-12]. Also, the fracture energies of epoxies have been reported to be a factor of 2 to 3 times greater than the expected theoretical estimate for purely brittle fracture[1,2,7,8,13-21].

We have investigated by optical and scanning electron microscopy the fracture topographies of amine-cured epoxies fractured in tension as a function of temperature, strain-rate, chemical composition and environmental exposure[9-12,22,23]. The topographical features indicate that microscopic flow can occur in these epoxies and that such flow can involve either crazing and/or shear banding.

In this paper we review evidence for the occurrence of microscopic flow under tensile loads, and discuss the nature of the microscopic deformation and failure modes in amine-cured epoxies. This evidence includes (i) optical and scanning electron microscopy studies of the fracture topographies of a variety of amine-cured epoxies that include both wet and dry specimens fractured as a function of temperature and strain-rate, (ii) bright-field transmission electron microscopy studies of thin films strained directly in the electron microscope[9,11] and (iii) birefringence studies of fractured specimens. The ability of amine-cured epoxies to undergo microscopic flow is discussed in terms of the physical and chemical nature of the epoxy network structure and how this structure can be modified under stress.

* This work was performed under the auspices of the US Department of Energy by Lawrence Livermore National Laboratory under Contract No W-7405-Eng-48

EXPERIMENTAL

Materials

Pure bisphenol-A-diglycidyl ether epoxide monomer (DGEBA) DER 332 (Dow) was the primary epoxide used in this study. The following amine curing agents were used (1) an aliphatic polyether triamine, Jeffamine T-403 (Jefferson), (2) 2,5 dimethyl 2,5 hexane diamine (DMHDA) (Aldrich), (3) *m*-phenylene diamine (MPDA) (Eastman) and (4) diethylene triamine (DETA) (Eastman). A polyamide Versamid 140 (General Mills) was also used as a curing agent. For each epoxy system a minimum of three glasses were prepared from (i) the stoichiometric epoxide: amine ratio, (ii) 15% excess epoxide and (iii) 15% excess amine.

Diaminodiphenyl sulfone (Ciba-Geigy, Eporal)-cured tetraglycidyl 4,4' diaminodiphenyl methane (Ciba Geigy MY720) epoxies (TGDDM–DDS) were also investigated. This epoxy is one of the most common systems used as a matrix for high performance composites. Both 'in-house' prepared TGDDM–DDS epoxies and commercially available epoxies whose primary constituents are TGDDM and DDS were investigated. The commercially

0032-3861/82/020295-11$03.00

Table 1 Cure conditions and T_g's of epoxies

Epoxy	Stoichiometric wt % of curing agent	Cure conditions	T_g (°C)
DGEBA–T–403	31	16 h 85°C	92 (25)
DGEBA–DMHDA	16	1 h 60°C, 3 h 130°C	142 (26)
DGEBA–MPDA	14	2 h 85°C, 24 h 150°C	155 (27)
DGEBA–DETA	11	24 h 23°C, 24 h 150°C	130 (28)
DGEBA–Versamid 140	31	24 h 23°C, 24 h 150°C	80 (29)
TGDDM–DDS	37	3 h 75°C, 1 h 150°C 5 h 177°C	225 (12)
TGDDM–DDS–5208	~21*	1 h 120°C, 2.5 h 177°C	206* (30)
TGDDM–DDS–934	~25*	1 h 120°C, 2.5 h 177°C	230* (30)

* Non-stoichiometric amounts of amine

available epoxies studied were Narmco 5208, which does not contain any catalyst, and Fiberite 934 which contained ~0.4 wt % BF_3 catalyst[24]. The cure conditions, the stoichiometric wt % of curing agent and the T_g's of the epoxies prepared from stoichiometric quantities of epoxy and amine are shown in *Table 1*. (The stoichiometric compositions were determined by assuming that all amine hydrogens react with epoxide groups in the absence of side reactions.) Prior to mixing, both the DGEBA and the amine monomers were exposed to vacuum to remove absorbed water. The DGEBA epoxy monomer was also heated to 60°C to melt any crystals present[10] and then was immediately mixed with the curing agent. The cure procedures utilized for the TGDDM–DDS epoxies were similar to those developed by Fanter[31].

Sheets of each epoxy system were prepared between glass plates separated by Teflon spacers. The epoxy sheets were either 0.75 or 3.0 mm thick. Release agents were used to facilitate the removal of the epoxy sheets from the glass plates. Dogbone-shaped specimens, suitable for tensile fracture were machined from the sheets and the edges of the specimens were polished along the gauge length. The 3.0 mm thick sheets were cut into dogbones with a gauge length of 5 cms and a width of 1.25 cms within the gauge length, whereas the thinner 0.75 mm thick sheets had a gauge length of 2.5 cms and a 0.3 cm width within the gauge length.

Experiments

For the fracture topography studies, the dogbone-shaped specimens were fractured in tension in a mechanical tester (Instron TTDM) in the crosshead speed range of 0.05 to 5.0 cm min^{-1} and from 23° up to 250°C. Each epoxy glass was studied at least at 3 temperatures at least in the 23° to $T_g - 25$°C range. A scanning reflection electron microscope (*SEM*) (Coates and Welter) and an optical microscope (Zeiss) were used for the fracture topography studies. For the *SEM* studies, the fracture surfaces were coated with gold while the sample was rotated in vacuum. A polarimeter (Photoelastic Inc.) and attached camera were used to record the birefringence of failed specimens.

RESULTS AND DISCUSSION

Overall fracture topography features

The fracture topographies of the epoxies that failed in tension can be divided into three characteristic regions (i) a coarse initiation region, (ii) a slow crack-growth, smooth region and (iii) a fast crack-growth, rough region. The characteristics of these regions can vary with test temperature, strain rate and chemical composition. In the following discussion these regions will be considered in terms of the microscopic deformation and failure modes.

Slow crack-growth fracture topographies associated with crazing

The sizes of the coarse initiation regions of the fracture topographies of amine-cured epoxies varied from 25 to 600 μm but generally were in the 25–50 μm diameter range. These regions were generally larger for the thinner epoxy specimens fractured at either higher temperatures or lower strain-rates and for the most part were circular in shape. However, the larger coarse initiation regions exhibited a more elongated ellipsoidal shape. The extremities observed in the dimensions and shapes of these coarse regions are illustrated in *Figures 1(a)* and *(b)*.

Although we systematically studied the coarse initiation regions as a function of stoichiometry, temperature and strain rate for each epoxy system we did not observe definite, systematic variations in these topographies as a function of these parameters. Indeed, the initiation topographies exhibited little consistency for similar epoxy glasses tested under the same conditions. This lack of consistency suggests that the flaw characteristics of these glasses and their associated stress fields under load play a primary role in the crack initiation processes. A typical range of topographies consisted of a nodular structure (*Figure 2*), a collapsed fibrillar topography (*Figure 3*) and a mica-like structure (*Figure 4*). Some initiation topographies also exhibited a porous texture as a result of crack propagation through a series of interconnected microvoids (*Figure 5*). At temperatures nearer the T_g, the fracture initiation regions are often much smoother than at lower fracture temperatures.

The coarse initiation region generally exists within a cavity. This coarse region can cover the entire surface of the cavity which itself is surrounded by a smooth, flat mirror-like region, or can be found at the centre of a penny-shaped cavity which exhibits a well-defined cusp at its circular periphary (*Figure 6*). *Figure 6(a)* exhibits a whole penny-shaped cavity because fracture initiated from an internal stress concentrator, whereas in *Figure 6(b)* only a portion of the cavity is present because initiation occurs from a surface defect. These penny-shaped topographies, which are observed as depressions on both the matching fracture surfaces, are produced from crack-propagation through shallow diamond-shaped cavities which are thickest at their centres. The shallow-walls of the penny-shaped cavities can exhibit distinct radial river-markings (*Figure 6(a)*) or essentially a smoother topography as exhibited in *Figure 6(b)*. The topographies surrounding the penny-shaped cavities are irregular and rough and are associated with fast-crack propagation. The diameters of the penny-shaped cavities are in the 250–1, 250 μm range, with sizes generally being nearer 1000 μm in diameter. The majority of the fracture topographies studied exhibited only one initiation region and associated cavity. However, occasionally multiple cavities are observed on the fracture surfaces of epoxies. *Figure 7* illustrates such multiple cavities on the fracture surface of a partially cured DGEBA-Versamid 140 (20 wt % Versamid 140) epoxy that is plasticized by unreacted DGEBA epoxide monomer[10]. Microclusters of the

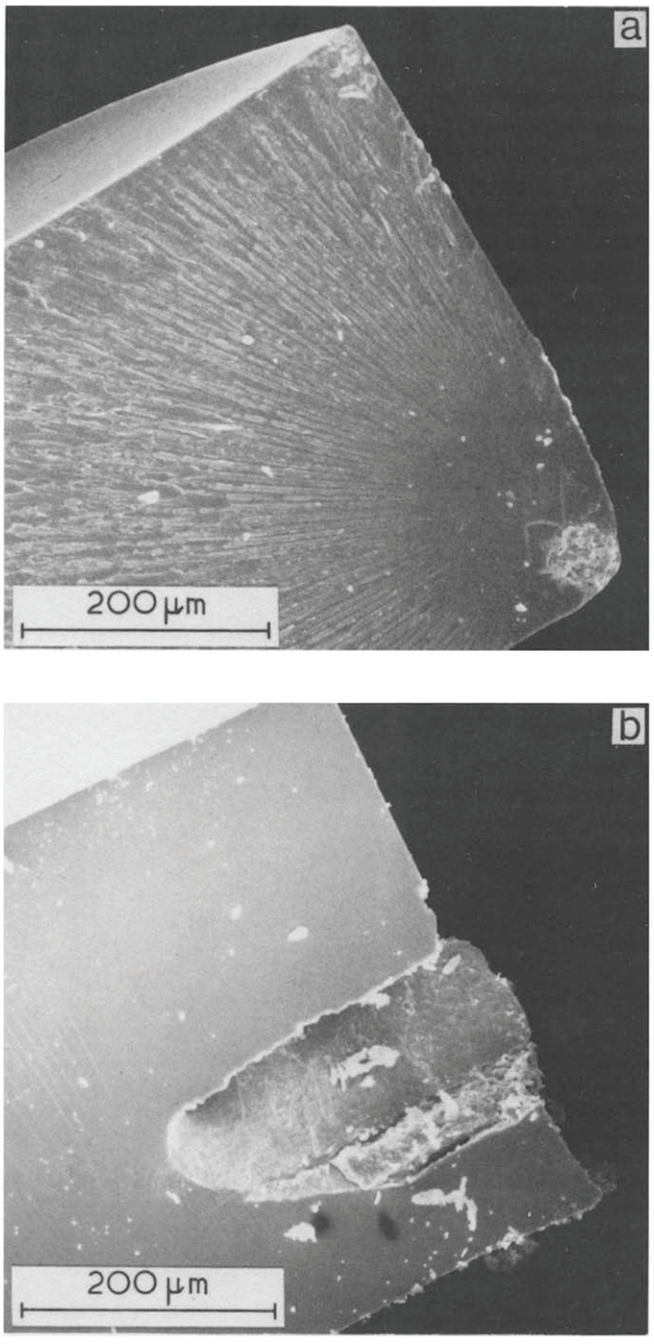

Figure 1 Scanning electron micrographs of coarse initiation regions in the fracture topographies of (a) TGDDM–DDS (27 wt % DDS) epoxy fractured at 23°C and (b) TGDDM–DDS (35 wt % DDS) epoxy fractured at 250°C

unreacted epoxide serve as initiation sites for multiple cavity formation.

The smooth, mirror-like fracture topographies that surround the coarse fracture topography initiation regions have been associated with slow crack growth and their areas increase with increasing temperature and moisture content, and decreasing strain rate[9-12,22,23]. These topographies exhibit a minimum at the epoxide: amine stoichiometric ratio. These smooth regions can extend over the whole fracture surface if the epoxy is fractured near its T_g. Previous fracture topography studies on non-crosslinked polymer glasses have found that such smooth, mirror-like regions also increase with increasing molecular weight[32-35]. Often these smooth topographies do contain radial river markings that originate from the coarse initiation regions (see *Figures 1*, *6*, and *7*). The river markings, which vary inconsistently from one epoxy specimen to another, are steps formed by the subdivision of the main crack into segments running on parallel planes.

The fracture topography initiation features described above for amine-cured epoxies can be explained in terms of a crazing process that precedes crack propagation. Murray and Hull[36] have reported that void growth and coalescence within a craze produce a planar cavity whose thickness is that of the craze. A mica-like structure in the slow crack-growth fracture topography of polymer glasses is generally associated with crack propagation through pre-existing craze material[37]. Murray and Hull[36] and Cornes and Haward[38] have both observed coarse topographies within initiation cavities in polystyrene and

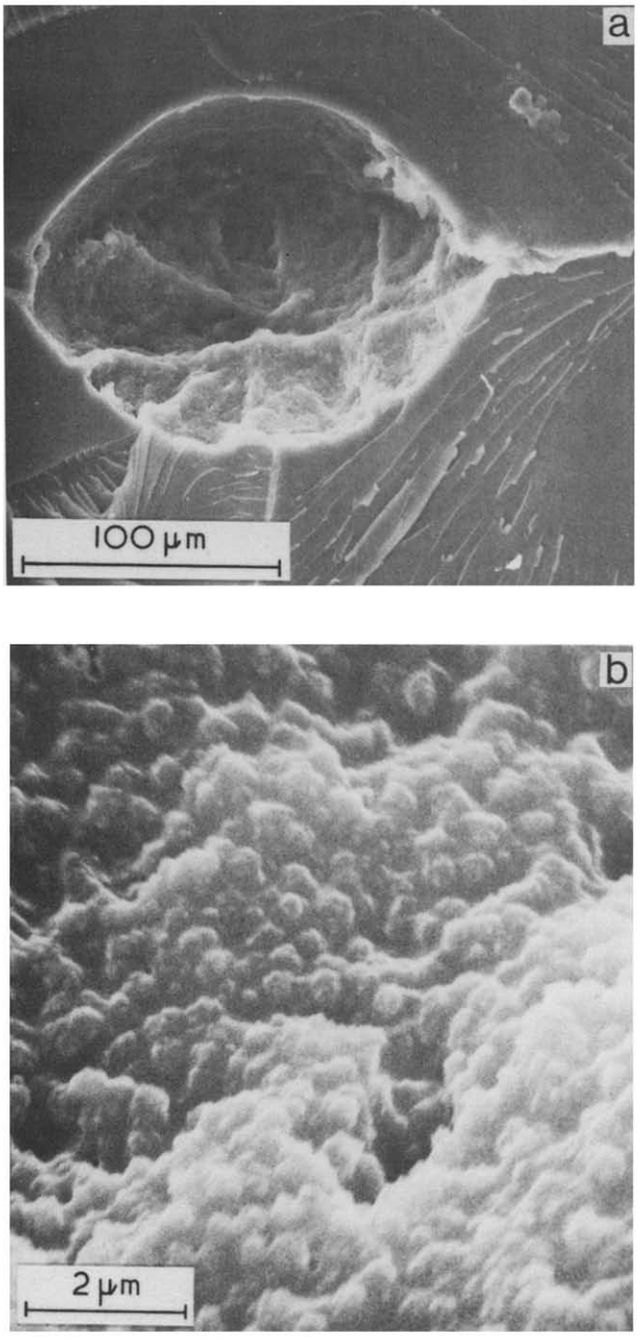

Figure 2 Scanning electron micrographs of (a) initiation cavity and (b) the nodular topography within the cavity; in a DGEBA–DETA (11 wt % DETA) epoxy fractured at 23°C

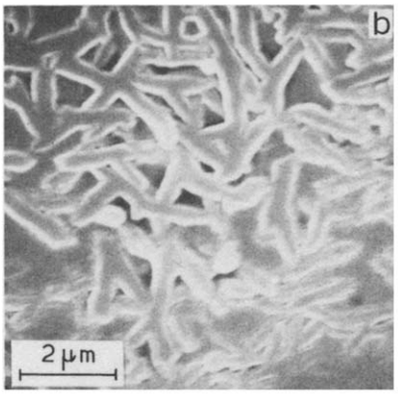

Figure 3 Scanning electron micrographs of the collapsed fibrillar topographies in the initiation regions of (a) DGEBA–DMHDA (16 wt % DMHDA) epoxy fractured at 75°C and (b) TGDDM–DDS (23 wt % DDS) epoxy fractured at 200°C

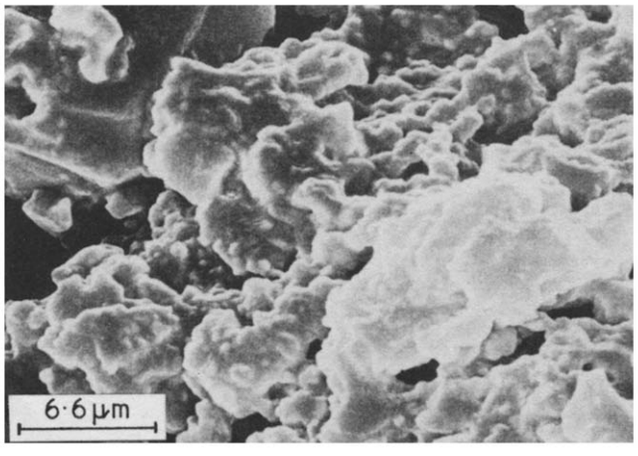

Figure 4 Scanning electron micrograph of the mica-like topography in the initiation region of a DGEBA–Versamid 140 (20 wt % Versamid 140) epoxy fractured at 23°C

poly(vinyl chloride), respectively. From studies on polystyrene, Murray and Hull[39] and Beahan *et al.*[40] have presented evidence that the initial stages of void growth and coalescence within a craze involve fracture through the centre of the craze. Furthermore, the coarseness of the craze fibrils has been reported to decrease with increasing craze width and thickness[40]. These observations suggest that the coarse initiation region in epoxies results from void growth and coalescence through the centre of a simultaneously growing, poorly developed craze which consists of coarse fibrils. The diameter of the broken fibrils depends on the relative rates of craze and void growth. The fibrillar structures that lie parallel to the fracture surface and the nodular topographies are associated with fractured craze fibrils. Doyle[41,42] and Hoare and Hull[43] have observed fractured fibrils that lie parallel to the fracture surface in polystyrene and have suggested that these fibrils are swept down onto the fracture surface as the crack passes through the craze. However, the mica-like topography that is observed in the initiation region more likely results from the coalescence of a bundle of parallel microcrazes situated in slightly different planes rather than exclusively from the fracture of poorly formed,

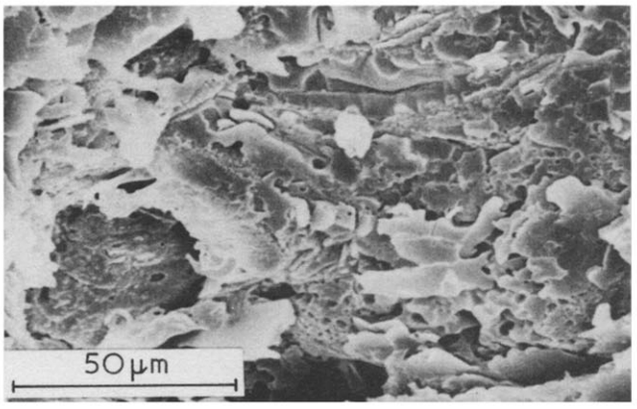

Figure 5 Scanning electron micrograph of microvoids in the fracture topography initiation region of TGDDM–DDS–5208 epoxy containing 4 wt % sorbed moisture that was fractured at 23°C

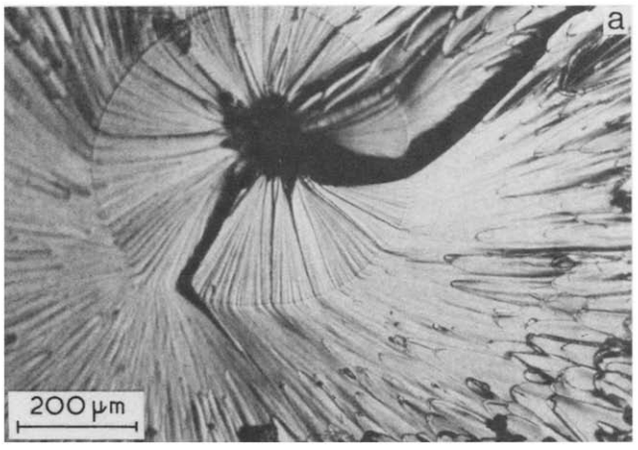

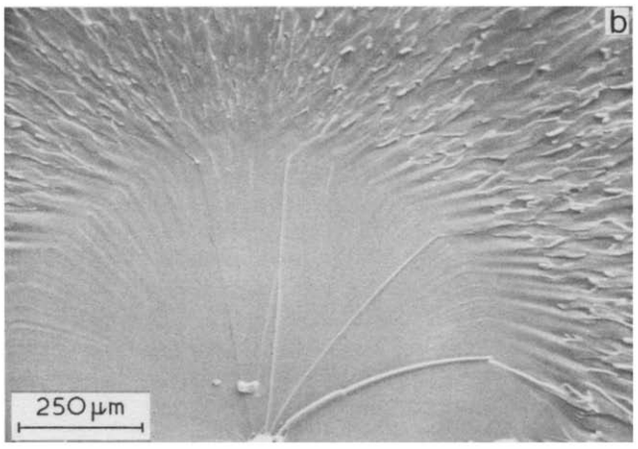

Figure 6 Penny-shaped cavities in the fracture topography initiation regions of (a) DGEBA–Versamid 140 (33 wt % Versamid 140) (optical micrograph) and (b) DGEBA–T–403 (31 wt % T–403) (scanning electron micrograph) epoxies fractured at 23°C

coarse fibrils. Skibo *et al.*[44] suggested that the mica-like structure which they observed in the non-initiation region of the fatigue–fracture topography of polystyrene is a result of the intersection of the crack plane with craze bundles. We also cannot preclude that any heterogeneous distribution in the crosslink density of the epoxy network[9-12] on a scale sufficient to allow preferential deformation and failure paths within the epoxy glass could be partially responsible for the observed coarse initiation topographies.

Recent studies of isolated crazes in thin polystyrene films by transmission electron microscopy (*TEM*) by Lauterwasser and Kramer[45] have led to new insights in understanding the crazing mechanism. Such observations have an important bearing in interpreting the slow crack-growth fracture topographies of epoxies. From a series of micrographs taken along the craze, Lauterwasser and Kramer[45] determined the craze thickness profile. Optical densitometry measurements of these micrographs were used to determine the fibril volume fractions and extension ratio at intervals along the craze. The craze surface stress profile and true stress in the craze fibrils were also computed from these experimental observations. The fibril extension profile along the craze was found to decrease from the craze tip to the craze centre indicating that in this case the craze thickened primarily by drawing new polymeric material across the craze surface into the fibrils rather than by creep of existing fibrils. Lauterwasser and Kramer[45] note that extension of the drawn craze fibrils will be a function of the craze surface stress at the time the fibrils are drawn. The surface stress profile was found to exhibit a slight maximum at the craze tip and decrease slowly away from the tip to $\sim 10\%$ below the applied stress field (see *Figure 8*). Lauterwasser and Kramer[45] claim the drawing of the fibrils at higher stresses just behind the growing craze tip results in the formation of a midrib which is a plane of fibrils with higher extensions situated midway between the craze surfaces. These observations and conclusions drawn by Lauterwasser and Kramer[45] can be utilized to further elucidate our understanding of the tensile failure processes of epoxies.

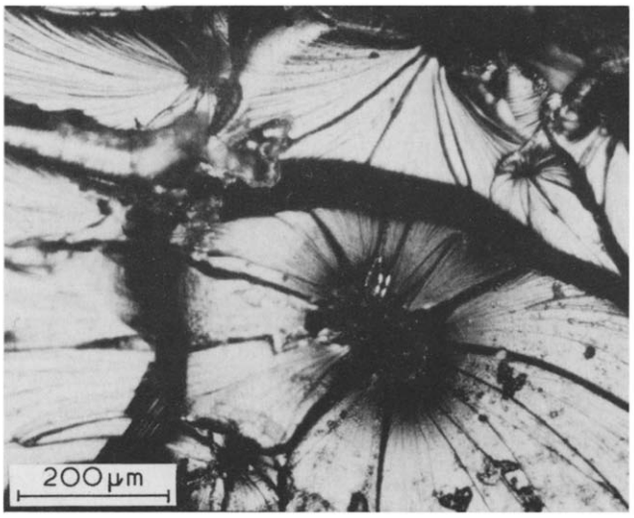

Figure 7 **Optical micrograph of multiple cavities in the fracture topography of partially cured DGEBA–Versamid 140 (20 wt % Versamid 140) that was fractured at 23°C**

In *Figure 8* we schematically illustrate four stages of failure in epoxies under an increasing tensile load. In each stage we document the craze/crack structure, the stress at the craze/crack surface and the resultant fracture topography.

In the first stage of failure a craze will grow in the epoxy glass under tension. A midrib of more highly oriented fibrils will develop within the craze. During the second stage of failure a crack will proceed through the craze midrib producing a rough fracture topography initiation region. (The generally observed 25–50 μm diameter size of these rough initiation regions indicates that the crazes grow to less than these dimensions prior to crack growth initiation.) Lauterwasser and Kramer[45] have noted that the crack will impose a high stress on the craze immediately ahead of the crack tip as illustrated in the second failure stage in *Figure 8*.

In the third stage of failure (*Figure 8*) the crack approaches the craze tip and imposes a higher stress field on the flaw tip region to produce a small plastic zone which results in a smooth fracture topography. The plastic zone ahead of the crack tip generally does not develop any of the characteristics of a craze in terms of void formation and fibrillation. Indeed, in *TEM* studies of deformed, thin glassy films of epoxies[9], polycarbonate[46-48] and polystyrene[45] regions of thinned

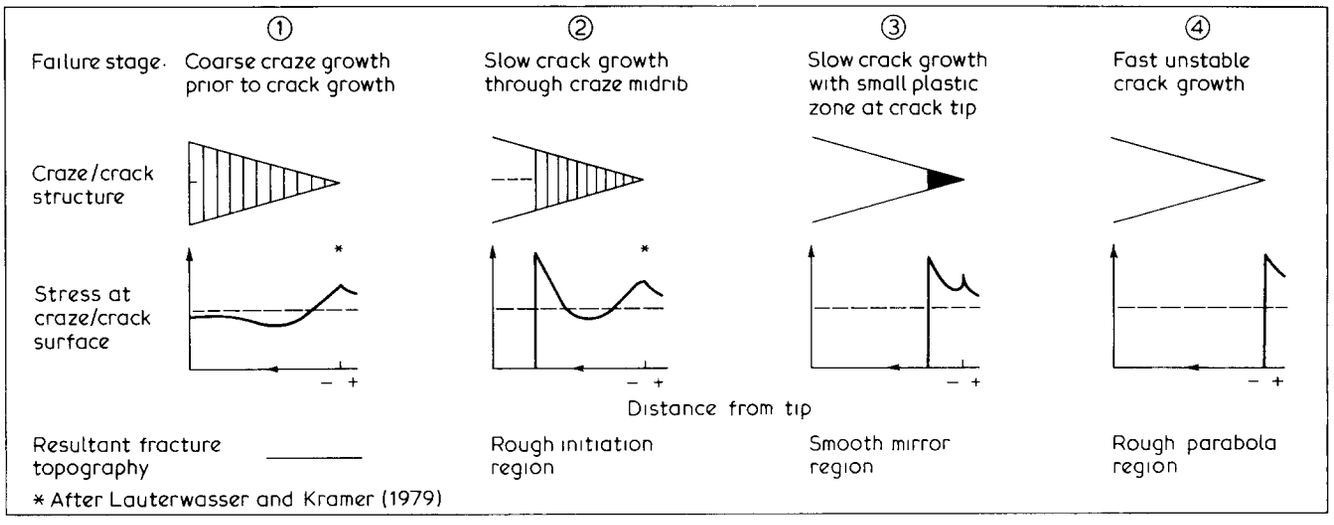

Figure 8 **Microscopic failure processes in epoxies in tension**

material that exhibit no detectable microvoids or fibrils have been observed at the tips of crazes. Such regions extend 300–600 nm in length with craze thicknesses of 4 to 900 nm. Similar regions at the tips of cracks in elastomers of 1–3 nm in length have been predicted by Schapery[49]. Furthermore, interference colours often observed in the mirror fracture topography regions of non-crosslinked polymer glasses[50] were not detected in such regions in epoxies. The absence of interference patterns further suggests that the thickness of the deformed layer was not large enough to cause interference with visible light. The smooth regions are, however, the result of plastic deformations at the crack tip because such regions increase with increasing test temperature, decreasing strain rate and the presence of moisture which acts as a plasticizer[9,11,12,23].

In the final stage of failure the crack propagates rapidly enough so that there is insufficient time for permanent, plastic deformation to occur at the crack tip.

The fracture topographies of epoxies do not exhibit the mackeral or patch topographies that are observed on the failure surfaces of thermoplastics[39,40,48,51–53]. Such topographies are associated with the crazing process. Lauterwasser and Kramer[45] suggest these topographies result from the following mechanism. In the second stage of failure illustrated in *Figure 8* a crack that propagates through the craze imposes a high stress field on the craze immediately ahead of the crack tip. The new craze fibrils that are drawn across the craze–matrix interfacial boundary under this higher stress field will have high extensions[45]. The presence of this highly oriented material at the craze boundary can cause the crack to propagate along the craze boundaries rather than through the midrib. In thermoplastics the crack can jump from one craze boundary to another in a regular manner producing a mackeral fracture topography or in an irregular fashion resulting in a patch topography[39,40,48,51–53]. The absence of these topographies in epoxies is a result of both small craze dimensions at the time when the crack initiates within the craze, and the subsequent relative rates of craze and crack propagation. The presence of crosslinks in epoxies will inhibit molecular flow and craze propagation compared to the more ductile non-crosslinked thermoplastics and these crosslinks will also enhance crack propagation through the less extensible craze fibrils. These phenomena will result in the crack tip rapidly catching-up to the craze tip and thus eliminating the possibility of highly oriented fibrils forming at the craze–matrix boundary interface and the resultant formation of a patch mackeral fracture topography.

Hence, fracture topography studies of a variety of amine-cured epoxies fractured in tension as a function of temperature and strain rate indicate that coarse craze structures can grow in epoxies under tensile loads. The slow crack growth fracture topography region consists of an initial rough region that can contain microvoids and/or fibrils followed by a smooth, temperature and strain rate-dependent region. Such topographies are explained by the initial formation of crazes. The crazes that can form in epoxies are less concentrated, smaller, less well defined and difficult to detect visually relative to those that grow in thermoplastics. Whether crazes occur under tension in a specific epoxy glass depends on a number of factors and their complex interaction. The ability of an epoxy network in the glassy-state to undergo molecular flow depends on the chemical and physical structure of the network and how this structure is modified by applied stress. (We will consider these structural aspects in a later section.) The specimen thickness will also play a role because thicker specimens inherently contain larger fabrication stresses and strains which can modify craze initiation and propagation. The specimen thickness will also modify plane strain-plane stress effects at the growing flaw tip.

A number of recent studies have been conducted on the fracture of epoxies under conditions of controlled crack propagation[54–60]. Notched specimens with a geometry such as a tapered double cantilever beam have been used to control crack propagation. In these studies it was found that for conditions that favoured molecular flow at the crack tip such as low strain rates, high temperatures or the presence of moisture, which acts as a plasticizer, crack propagation in epoxies tends to become unstable and occur in a 'slip-stick' manner. Such phenomena lower the yield stress at the crack tip thus promoting molecular flow which favours crack blunting and a 'slip-stick' behaviour. The stress fields at the notch tips in these controlled crack propagation test specimens would generally be higher than those stress fields associated with natural flaws in un-notched specimens and as such would be less favourable towards coarse craze formation. Notched specimens would be more likely to immediately favour a small plastic zone at the crack tip (third stage of failure illustrated in *Figure 8*) and bypass significant coarse craze formation completely. Indeed, Gledhill and Kinloch[67], Mijovic and Koutsky[58], and Yamini and Young[60] report no evidence of crazing in their fractured notched specimens. Smooth mirror fracture topographies were found in specimens that failed by continuous crack propagation[54,56,59,60], whereas crack arrest lines were observed when a 'slip stick' mode occurred. The smooth topographies are expected for a small plastic zone ahead of the crack tip. Whether this plastic flow at the crack tip occurs by shear yielding or yielding under normal stresses is difficult to ascertain experimentally for small plastic zones and will depend on the stress fields imposed on the epoxy immediately ahead of the crack tip.

Yamini and Young[60] have claimed the smooth featureless topographies in these notched specimens presents overwhelming evidence against craze growth in epoxy glasses. However, Yamini and Young[60] limit their evidence to relatively thick notched specimens and make no attempt to explain the fracture topographies of un-notched tensile specimens of different thicknesses that we have reviewed in this paper.

Fracture topography initiation regions associated with shear banding

The fracture topography features in the initiation regions of TGDDM–DDS epoxies indicate that shear banding can occur in these glasses. These epoxies were prepared in silicone rubber moulds by fabrication techniques developed by Fanter[31]. Such specimens exhibited uniform, optical anisotropy under polarized light indicating the epoxy networks are structurally anisotropic. This anisotropy may favour the more directional shear band propagation mode relative to the craze process. (Other amine-cured epoxies investigated in this study did not exhibit fracture topography initiation features associated with shear banding. These epoxies

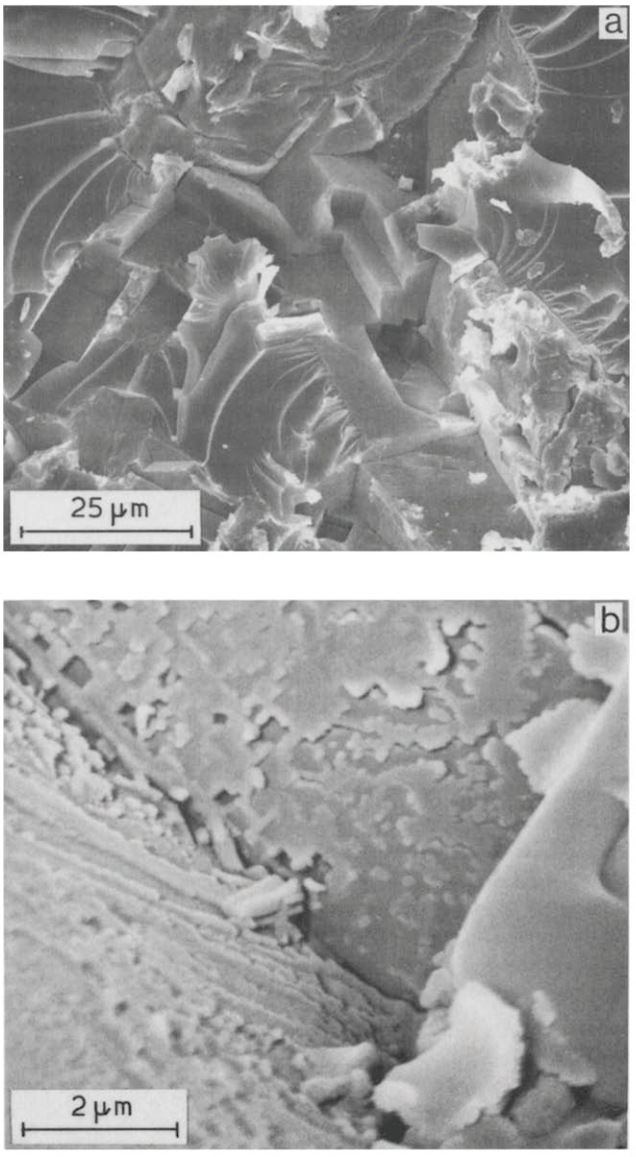

Figure 9 **Scanning electron micrographs of multiple right-angle steps in the fracture topography initiation regions of TGDDM–DDS (35 wt % DDS) epoxy fractured at 225°C**

were not formed in silicone moulds and did not exhibit optical anisotropy.)

The TGDDM–DDS epoxies exhibited multiple right-angle steps in their fracture topography initiation regions, as illustrated in *Figure 9(a)*[12]. The planes of these steps were generally found to be at an angle of ~45° with the overall fracture plane. The topographies of these right-angle steps exhibit a finer structure at higher magnifications. The faces of a right-angle step and their in line intersection, which intersects the top left-corner of the micrograph, are illustrated in *Figure 9(b)*. Attached to each face is ~100 nm thick, deformed layer of polymer which consists of rectangular-shaped voids and protrusions with dimension of 100 to 500 nm. The voids and protrusions generally are aligned parallel to the line at which the larger perpendicular planes intersect.

These unusual topographies we believe are a result of shear bands propagating at 45° to the applied tensile load direction and intersecting at right-angles. The shear deformation will produce structurally weak planes in these crosslinked glasses as a result of bond cleavage. The intersection of shear bands can cause a stress concentration[61,62] that is sufficient to promote crack propagation through the structurally weak planes formed by shear band propagation. These phenomena produce the unique multiple right-angle steps observed in the fracture topography of TGDDM–DDS epoxies. The fine rectangular structures observed on the surfaces of the larger shear band planes suggests that these bands consist of packets of micro-shear bands, which have been observed by Wu and Li in their studies on polystyrene[63]. Further evidence that these topographies are a result of shear band propagation is that they become more prevalent at higher temperatures[12] which is consistent with the shear band mode of deformation becoming more favoured relative to the crazing mode with increasing temperature[53,64,65].

Step-like fracture topographies are also observed in the faster crack propagation region of epoxies[58] and phenol-formaldehyde resin[4], but should not be confused with the multiple right-angle steps that we observe in the fracture topography initiation regions of TGDDM DDS epoxies. This step-like topography is illustrated in *Figure 10(a)* in the faster crack propagation region of a DGEBA–DMHDA epoxy. These steps are caused by a relatively brittle cleavage fracture process[66] in which a periodic change in the crack front plane occurs. A fibril or a thin layer of epoxy is often formed at the step where the crack front jumps into a different plane. Such fibrils are illustrated in *Figure 10(a)* and are shown in more detail in *Figure 10(b)*. We emphasize that these cleavage steps are not a result of the shear band deformation process we observe in the

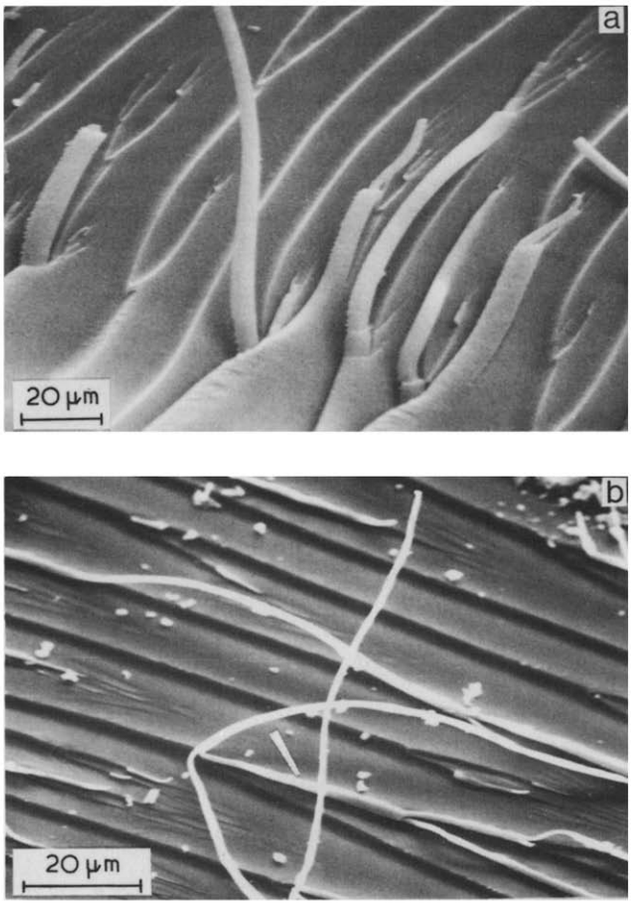

Figure 10 **Scanning electron micrographs of cleavage steps and associated fibrils in the faster crack propagation regions of DGEBA–DMHDA (16 wt % DMHDA) epoxies fractured at 23°C**

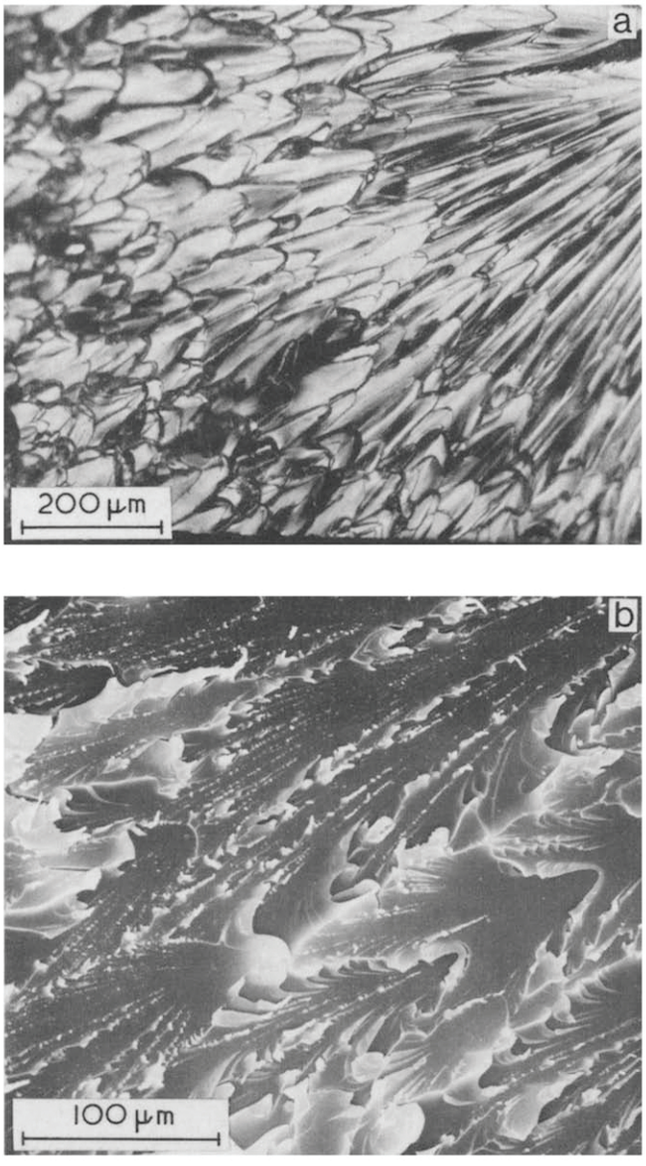

Figure 11 **Fast crack fracture topographies in (a) DGEBA–Versamid 140 (31 wt % Versamid 140) epoxy fractured at 23°C (optical micrograph) and (b) DGEBA–MPDA (14 wt % MPDA) fractured at 100°C (scanning electron micrograph)**

fracture topography initiation region. These steps do not form in the fracture topography initiation region, are not situated at ~45° to applied tensile load direction and, indeed, become less prevalent with increasing temperature and/or decreasing strain rate.

Fast crack growth fracture topographies

The fast crack, rough fracture topographies that occur in amine-cured epoxies that failed in tension are a result of complex, unstable, brittle fracture. The energy involved in this brittle fracture will be considerably smaller than that associated with the plastic deformations that occur at slower crack velocities. The areas of these rough topographies on the fracture surfaces increase with decreasing temperature and increasing strain rate as plastic deformations at the crack tip become more difficult.

The micrographs in *Figure 11* illustrate typical rough, fast crack topographies observed in epoxies. The optical micrograph in *Figure 11(a)* illustrates numerous parabolas, whereas more complex topographical features are illustrated at higher magnifications in the *SEM* in *Figure 11(b)*. The surface roughness is primarily caused by the generation of secondary crack fronts ahead of the primary crack front and the interconnection of these fronts from different fracture planes. The high stresses generated ahead of the primary crack front initiate secondary cracks at stress-raising material inhomogeneity sites within the epoxy. The shapes generated on the fracture surface by the interaction of primary and secondary crack fronts in brittle amorphous materials, such as the parabolic shapes illustrated in *Figure 11(a)*, have been explained by Lednicky and Pelzbauer[67] in terms of the velocities of the fracture fronts and their distance apart. The fracture topographical features are further complicated by crack bifurcations and complex, dynamic interactions of shock waves, released during fracture, with the propagating crack fronts. Occasionally we have observed distinct Wallner lines[68] which are formed at the loci of the primary crack front with transverse shock waves, but generally the topographies of the fast crack propagation regions of the epoxies are too complex to interpret in detail.

Further evidence of plastic flow

In addition to the fracture topography observations in the slower crack propagation regions of epoxies a number of additional observations also indicate permanent molecular flow can occur in amine-cured epoxy networks in the glassy state.

Amine-cured epoxies can exhibit macroscopic tensile yield stresses in the glassy state[11,28]. Such yield stresses exhibit similar free volume dependencies as a function of thermal history as non-crosslinked glasses such as polycarbonate[11,28,53]. From Eyring's theory of stress-activated viscous flow in polymers[69] the strain rate and temperature dependencies of the epoxy yield stresses produce activation volumes associated with chain segment jumps similar in magnitude to those volumes associated with flow in non-crosslinked glasses[28]. Furthermore, many of the amine-cured epoxies we have studied exhibit ultimate elongations in the 10–30% range in the glassy state[11,12,28].

TEM and birefringence studies of strained and/or fractured epoxies have revealed more direct experimental evidence that molecular flow can occur in these glasses. Films of DGEBA–DETA (~11 wt % DETA) epoxies, ~1 μm thick, were strained directly in the electron microscope and the deformation processes were observed in bright-field *TEM*[9,11]. Coarse craze fibrils yielded inhomogeneously by a process that involved the movement of indeformable 6–9 nm diameter, highly crosslinked molecular domains past one another. The material between such domains yielded and became thinner as plastic flow occurred. Plastic deformations have also been observed from birefringence studies of 3 mm thick tensile specimens of DGEBA–DMHDA (16 wt % DMHDA) and DGEBA–T-403 (31 wt % T-403) epoxies. Fractured DGEBA–DMHDA (16 wt % DMHDA) epoxies exhibited birefringent patterns in their gauge length's after fracture at ≥75°C as illustrated in *Figure 12*. (Prior to tensile deformation these epoxy specimens did not exhibit birefringence.) Regions of 'frozen-in' homogeneous strain, as indicated by a uniform colour under polarized white light, were observed in these fractured epoxies. In such regions the epoxy networks have undergone homogeneous plastic deformation.

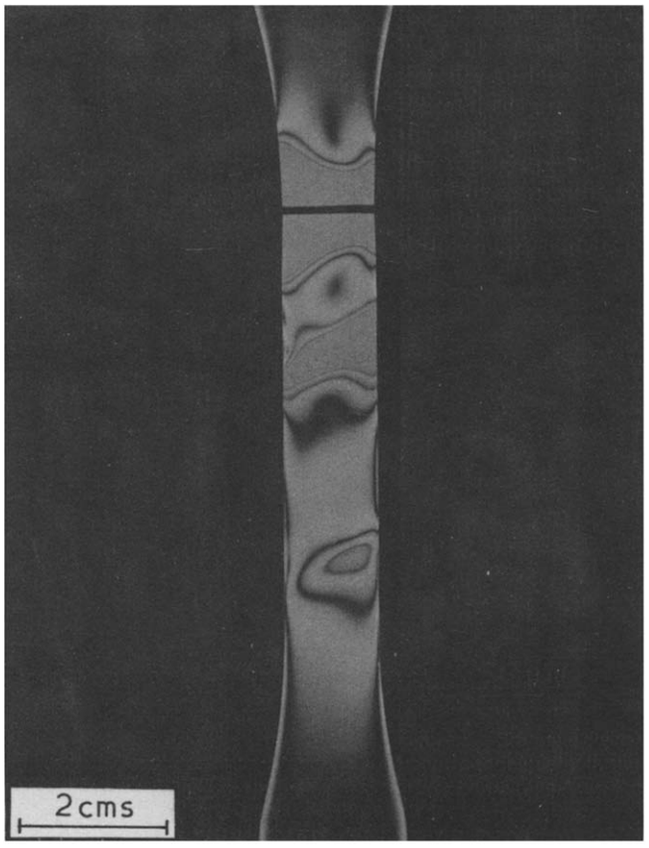

Figure 12 **Optical micrograph under polarized light of a fractured DGEBA–DMHDA (16 wt % DMHDA) epoxy that was fractured at 125°C**

Inhomogeneous regions of high strain also occur in these networks as indicated by concentrations of birefringent fringes which are shown in *Figure 12*. These regions of high strain gradients were observed to develop into diffuse shear bands which propagated at ~45° to the applied tensile load direction. In the case of DGEBA–T-403 (31 wt % T-403) epoxies plastic flow was directly observed to occur under increasing tensile load at room temperature. Regions of high strain gradients developed at each end of the specimen gauge length, some of which subsequently developed into diffuse shear bands, whereas the central portion of the gauge length deformed in a more homogeneous plastic manner.

Structural factors and mechanisms that allow flow to occur

The ability of crosslinked amine-cured epoxy networks to undergo microscopic flow in the glassy state could result from a number of structural phenomena and mechanisms.

Amine-cured epoxy networks are generally assumed to result exclusively from addition reactions of epoxide groups with primary and secondary amines[70]. However, networks of lower crosslink density, that will be more susceptible to molecular flow, are often formed as a result of incomplete cure reactions and/or epoxide homopolymerization[7,10–12,24,28,71–85].

Flow in epoxy glasses will also be enhanced in networks with heterogeneous crosslink density distributions in which regions of lower crosslink density form the continuous phase. However, the primary experimental evidence for heterogeneous regions of crosslink density in the 6–10 000 nm size range in thermosets is derived from electron microscope observations and is somewhat controversial[4,9,11,22,24,85–107].

On a smaller scale than the above heterogeneous regions of crosslink density the degree of network perfection in terms of the molecular weight between crosslinks, chain branches and loops also plays a critical role in the ability of the epoxy glass to undergo flow. A perfectly homogeneous crosslinked network can undergo homogeneous deformation by each segment between crosslinks extending to the same extent to form extended-chain configurations. This homogeneous deformation process will result in glasses of high ductility. Indeed, we have recently observed that more highly crosslinked but more perfectly homogeneous DGEBA–T-403 epoxy networks exhibit higher ductilities than lower crosslinked less perfect networks[108]. This homogeneous plastic deformation will be enhanced by the flexibility of the units between crosslinks and the free volume available to such segments. Network imperfections will lead to inhomogeneous deformations in the form of crazing and shear banding. In such regions of high local strain, chain scission and molecular pull-out will occur. However, chain scission can lead to a lower overall crosslink density within the epoxy network thus allowing flow to occur more easily. Indeed, epoxies have been reported to become tougher with time during static loading[56,59,109]. This self-toughening mechanism does suggest that chain scission can occur in epoxies under load. More direct experimental evidence has been reported by Levy and Fanter[110] who observed enhanced chemiluminescence in TGDDM–DDS epoxies under stress. This chemiluminescence is associated with bond fracture and subsequent reaction of the macro-radicals with oxygen.

CONCLUSIONS

A variety of evidence shows that plastic flow can occur under tensile loads in crosslinked amine-cured epoxy glasses. This flow can occur by homogeneous deformation, or inhomogeneously via crazing and/or shear banding. Cracks are often initiated in these glasses by a crazing process.

The slow-crack growth fracture topographies of a variety of amine-cured epoxies, fractured in tension as a function of temperature and strain rate consist of a rough initiation region, that can contain microvoids and/or fractured fibrils, surrounded by a smooth temperature and strain rate dependent region. These topographical features are a result of initial coarse craze formation followed by crack propagation through the craze midrib. The crack rapidly catches up to the craze tip and imposes a higher stress field on the tip which produces a small plastic zone that results in a smooth fracture topography. Flow in the fracture initiation region of epoxies can also occur to a lesser extent by shear band propagation which results in a topography of multiple right angle steps whose planes are situated at ~45° to the applied tensile load direction.

Further evidence that flow occurs in these epoxies is that in the glassy state they can exhibit macroscopic yield stresses and their ultimate elongations can be in the 10–30% range.

TEM and birefringence observations provide more direct experimental evidence of the deformation and failure processes of amine-cured epoxies. Coarse craze

formation and flow have been observed for an amine-cured epoxy film strained directly in the electron microscope. Birefringent patterns in deformed and fractured epoxies indicate both plastic homogeneous and, also, inhomogeneous deformations can occur in these glasses. The inhomogeneous deformations can evolve into macroscopic shear bands.

The ability of amine-cured epoxies to undergo microscopic flow will be enhanced by (i) incomplete cure reactions and/or epoxide homopolymerization, which results in a lower crosslinked density network, (ii) a heterogeneous crosslink density distribution within the epoxy network in which regions of low crosslink density form the continuous phase and control the flow processes, (iii) covalent bond scission under stress, which results in a lower crosslink density, (iv) chain flexibility and (v) high glassy-state free volume. Perfectly homogeneous crosslinked networks will favour homogeneous plastic deformation, whereas less perfect networks will favour inhomogeneous plastic deformations in the form of crazing and/or shear banding.

ACKNOWLEDGEMENTS

The authors wish to acknowledge Drs R. Christensen and L. E. Nielsen for their stimulating discussions related to these studies and Mr J. Stone for producing the optical micrograph of a fractured epoxy under polarized light.

REFERENCES

1 Broutman, L. J. and McGarry F. J. *J. Appl. Polym. Sci.* 1965, **9**, 609
2 Griffiths, R and Holloway, D. G. *J. Mater. Sci.* 1970, **5**, 302
3 Patrick, R. L., Gehman, W G , Dunbar, L. and Brown, J. A. *J. Adhesion* 1971, **3**, 165
4 Nelson, B E. and Turner, D. T. *J Polym. Sci. A-2* 1972, **10**, 2461
5 Bowden, P B. and Dukes, J. A. *J. Mater. Sci.* 1972, **7**, 52
6 Patrick, R. L. in 'Treatise on Adhesion and Adhesives', Vol 3 (Ed. R. L. Patrick) Dekker, New York, 1973, p 163
7 Young, R J. and Beaumont, P. W. R. *J. Mater. Sci.* 1975, **10**, 1343
8 Christiansen, A. and Shortall, J. B. *J. Mater. Sci.* 1976, **11**, 1113
9 Morgan, R. J. and O'Neal, J E *J. Mater Sci* 1977, **12**, 1966
10 Morgan, R J. and O'Neal, J. E. *J Macromol. Sci. Phys* 1978, **B15**, 139
11 Morgan, R. J and O'Neal, J. E. *Polym. Plast Techol Eng.* 1978, **10**, 49
12 Morgan, R. J., O'Neal, J. E. and Miller, D. B. *J Mater. Sci.* 1979, **14**, 109
13 Mostovoy, S. and Ripling, E. J. *J. Appl. Polym. Sci.* 1966, **10**, 1351
14 Mostovoy, S. and Ripling, E. J. *J. Appl. Polym. Sci.* 1971, **15**, 611
15 DiBenedetto, A. T. and Wambach, A. D. *Int. J. Polym. Mater.* 1972, **1**, 159
16 Diggwa, A. D. S. *Polymer* 1974, **15**, 101
17 Bascom, W. D , Cottington, R. L., Jones, R. L. and Peyser, P. *J. Appl. Polym. Sci.* 1975, **19**, 2545
18 Babayevskii, P. G. and Trostyanskaya, Ye. B. *Vysokomol. soyed.* 1975, **A17**, 906
19 Gledhill, R. A. and Kinloch, A. J. *J. Mater. Sci.* 1975, **10**, 1263
20 Bascom, W. D., Cottington, R. L. and Timmons, C. O. *J. Appl. Polym Sci. Applied Polymer Symposium* 1977, **32**, 165
21 Andrews, E. H and Stevenson, A *J. Mater. Sci.* 1978, **13**, 1680
22 Morgan, R. J and O'Neal, J E. in 'Chemistry and Properties of Crosslinked Polymers', (Ed S. S. Labana), 1977, Academic Press, New York, p 289
23 Morgan, R J., O'Neal, J. E and Fanter, D. L. *J. Mater. Sci.* 1980, **15**, 751
24 Morgan, R. J. and Mones, E. T. *Composites Tech. Rev.* 1979, **1**, No 4, 18
25 Rinde, J. A. 'DER 332/Jeffamine T-403 Cure Cycles', Fiber Composites Memo, Lawrence Livermore National Laboratory, 1977
26 Rinde, J. A., Chiu, I., Mones, E. T. and Newey, H. A. '2,5 Dimethyl 2,5 Hexane Diamine: A Promising New Curing Agent for Epoxy Resins', Lawrence Livermore National Laboratory, UCRL-82155, 1979
27 Lee, H. and Neville, K. 'Handbook of Epoxy Resins', McGraw-Hill, New York, Ch 8, 1967
28 Morgan, R. J. *J. Appl. Polym. Sci.* 1979, **23**, 2711
29 Lee, H. and Neville, K. 'Handbook of Epoxy Resins', McGraw-Hill, New York, 1967, Ch 10
30 Morgan, R. J., Mones, E. T. and Chiu, I. Unpublished Dynamic Mechanical Data
31 Fanter, D. L *Rev. Sci. Instrum.* 1978, **49**, 1005
32 Zandeman, F 'Publs. Scient. Tech. Minist. Air', Paris, No. 291, Ch IV, 1954
33 Newman, S. B. and Wolock, I. *J. Appl. Phys.* 1958, **29**, 49
34 Wolock, I. and Newman, S. B. in 'Fracture Processes in Polymeric Solids', (Ed. B. Rosen) Interscience, Ch IIc, 1964
35 Bird, R. J., Mann, J., Pogany, G. and Rooney, G. *Polymer* 1966, **7**, 307
36 Murray, J. and Hull, D. *Polymer* 1969, **10**, 451
37 Rabinowitz, S., Krause, A R. and Beardmore, P. *J. Mater. Sci.* 1973, **8**, 11
38 Cornes, P. L. and Haward, R. N. *Polymer* 1974, **15**, 149
39 Murray, J. and Hull, D. *J. Polym. Sci. Part A-2*, 1970, **8**, 1521
40 Beahan, P., Bevis, M. and Hull, D *J. Mater. Sci.* 1972, **8**, 162
41 Doyle, M. J. *J. Polym. Sci., Polym. Phys. Edn.* 1975, **13**, 127
42 Doyle, M J. *J. Mater. Sci.* 1975, **10**, 300
43 Hoare, J. and Hull, D. *J. Mater. Sci.* 1975, **10**, 1861
44 Skibo, M. D., Hertzberg, R W. and Manson, J. A. *J. Mater. Sci.* 1976, **11**, 479
45 Lauterwasser, B. D. and Kramer, E J. *Phil Mag. A*, 1979, **39**, 469
46 Wyzgoski, M. G. and Yeh, G. S. Y *J. Macromol. Sci-Phys.* 1974, **B10**, 647
47 Thomas, E. L and Israel, S. J. *J. Mater. Sci.* 1975, **10**, 1603
48 Morgan, R. J. and O'Neal, J. E. *Polymer* 1979, **20**, 375
49 Schapery, R. A. *Int J. Fract.* 1975, **11**, 549
50 Kambour, R. P. *J. Polym. Sci.* 1965, **A3**, 1713
51 Murray, J. and Hull, D. *J. Polym. Sci., A-2*, 1970, **8**, 583
52 Hull, D. and Owen, T. W. *J Polym Sci , Polym Phys. Edn.* 1973, **11**, 2039
53 Morgan, R. J. and O'Neal, J. E. *J. Polym. Sci., Polym. Phys. Edn.* 1976, **14**, 1053
54 Yamini, S. and Young, R. J. *Polymer* 1977, **18**, 1075
55 Gledhill, R. A., Kinloch, A. J., Yamini, S. and Young, R J. *Polymer* 1978, **18**, 574
56 Phillips, D. C., Scott, J. M. and Jones, M. *J. Mater. Sci.* 1978, **13**, 311
57 Gledhill, R. A. and Kinloch, A J. *Polym. Eng. Sci.* 1979, **19**, 82
58 Mijovic, J. and Koutsky, J. A. *Polymer* 1979, **20**, 1095
59 Kinloch, A. J. and Williams, J. G. *J Mater. Sci.* 1980, **15**, 987
60 Yamini, S. and Young, R. J. *J. Mater. Sci.* 1980, **15**, 1823
61 Hull, D. *Acta Met* 1960, **8**, 11
62 Mills, N J *J. Mater. Sci.* 1976, **11**, 363
63 Wu, J. B. C. and Li, J. C. M. *J. Mater. Sci.* 1976, **11**, 434
64 Sternstein, S. S and Ongchin, L. *Polymer Prepr (ACS)* 1969, **10**, 1117
65 Haward, R. N., Murphy, B. M. and White, E F. T. *J Polym. Sci. A-2*, 1971, **9**, 801
66 'Fractography and Atlas of Fractographs', Metals Handbook, Vol 9, (Ed. J. A. Fellows), American Society for Metals, Metals Park, Ohio, 1974, p 119
67 Lednicky, F. and Pelzbauer, Z. *Int. J. Polym. Mater.* 1973, **2**, 149
68 Wallner, H. *Z. Phys.* 1939, **114**, 368
69 Eyring, H. *J. Chem. Phys.* 1936, **4**, 283
70 Lee, H. and Neville, K. Handbook of Epoxy Resins, McGraw-Hill, New York, Ch 5 and 7, 1967
71 French, D. M., Strecker, R. A. H. and Tompa, A. S. *J. Appl. Polym. Sci.* 1970, **14**, 599
72 Horie, K., Hiura, H., Sawada, M., Mita, I. and Kambe, H *J. Polym. Sci. A-1*, 1970, **9**, 1357
73 Acitelli, M. A., Prime, P. B. and Sacher, E. *Polymer* 1971, **12**, 335
74 Prime, R. B. and Sacher, E *Polymer* 1972, **13**, 455
75 Whiting, D. A. and Kline, D. E. *J. Appl. Polym. Sci.* 1974, **18**, 1043
76 Lee, H. and Neville, K. 'Handbook of Epoxy Resins', McGraw-Hill, New York, 1967, Ch 5, 7, 8 and 9
77 Sidyakin, P. V. *Vysokomol. Soyed* 1972. **A14**, 979
78 Bell, J. P and McCavill, W. T. *J. Appl. Polym. Sci.* 1974, **18**, 2243
79 Anderson, H. C. *SPE Journal* 1960, **16**, 1241
80 Kakurai, T. and Noguchi, T *J Soc. Org. Syn. Chem Jpn.* 1960, **18**, 485

81 Kwei, T K. *J. Polym. Sci.* 1963, **A-1**, 2985
82 Tanaka, Y. and Mika, T F. in 'Epoxy Resins', (Eds C. A. May and Y. Tanaka), Marcel Dekker, Inc., New York, Ch 3, 1973
83 Dusek, K., Bleha, M. and Lunak, S. *J. Polym Sci., Polym Chem Edn.* 1977, **15**, 2393
84 Schneider, N. S., Sprouse, J. F., Hagnauer, G L. and Gillham, J K. *Polym. Eng. Sci.* 1979, **19**, 304
85 Erath, E. H. and Robinson, M *J. Polym. Sci. Part C*, 1963, **3**, 65
86 Wohnsiedler, H P. *J. Polym. Sci., Part C*, 1963, **3**, 77
87 Cuthrell, R E. *J. Appl. Polym. Sci.* 1967, **11**, 949
88 Solomon, D. H., Loft, B C. and Swift, J D *J Appl Polym. Sci* 1967, **11**, 1593
89 Kenyon, A S. and Nielsen, L E *J Macromol. Sci-Chem.* 1969, **A3(2)**, 275
90 Karyakina, M I., Mogilevich, M M., Maiorova, N. V and Udalova, A. V. *Vysokomol. Soedin* 1975, **A17**, 466
91 Luettgert, K E. and Bonart, R *Prog. Colloid. and Polym Sci* 1978, **64**, 38
92 Racich, J. L. and Koutsky, J. A. *J. Appl. Polym Sci.* 1976, **20**, 2111
93 Rochow, T. G. and Rowe, F. G. *Anal. Chem.* 1949, **21**, 261
94 Spurr, R. A., Erath, E. H., Myers, H. and Pease, D. C *Ind Eng Chem.* 1957, **49**, 1839
95 Erath, E. H. and Spurr, R. A. *J Polym. Sci.* 1959, **35**, 391
96 Rochow, T. G. *Anal. Chem.* 1961, **33**, 1810
97 Neverov, A N., Birkina, N. A Zherdev, Yu. V. and Kozlov, V A. *Vysokomol. Soedin.* 1968, **A10**, 463
98 Nenkov, G. and Mikhailov, M. *Makromol. Chem* 1969, **129**, 137
99 Basin, Ye. V, Konunskii, L. M., Shokalskaya, O. Y and Aleksandrov, N V *Polym Sci USSR.* 1972, **14**, 2339
100 Kessenikh, R M., Korshunova, L A. and Petrov, A V *Polym Sci. USSR* 1972, **14**, 466
101 Bozveliev, L G and Mihajlov, M. G. *J Appl Polym. Sci.* 1973, **17**, 1963 and 1973
102 Selby, K. and Miller, L E *J. Mater. Sci.* 1975, **10**, 12
103 Maiorova, M V., Mogilevich, M M., Karyakina, M. I and Udalova, A V *Vysokomol Soedin.* 1975, **A17**, 471
104 Smartsev, V M., Chalykh, A. Ye, Nenakhov, S. A and Sanzharovskii, A T. *Vysokomol. Soedin.* 1975, **A17**, 836
105 Manson, J. A, Sperling, J. H. and Kim, S L 'Influence of Crosslinking on the Mechanical Properties of High T_g Polymers', Technical Report, AFML-TR-77-109, 1977
106 Dusek, K., Plestil, J., Lednicky, F. and Lunak, S *Polymer* 1978, **19**, 393
107 Schmid, R *Prog Colloid and Polym. Sci* 1978, **17**, 64
108 Kong, F. M, Mones, E. T and Morgan, R J., unpublished
109 Gledhill, R A., Kinloch, A J. and Shaw, S. J. *J Mater. Sci.* 1979, **14**, 1769
110 Levy, R L. and Fanter, D. L. *Polym Prepr. (ACS)* 1979, **20(2)**, 543